

# Chapter 2

## Metamaterial-Based Miniaturized Planar Inverted-F Antenna

S. Manjula and Balamati Choudhury

### 2.1 Introduction

The fast-growing high-profile mobile communication systems demand miniaturization of mobile systems, which leads to the reduction in antenna size. The design of compact antennas with enhanced performance such as low specific absorption rate ( $c$ ), large bandwidth and multiband operation is gaining momentum. Efficient use of metamaterial structure has got great importance in this miniaturization process.

Planar inverted-F antennas (PIFA) are widely used in mobile applications as it is compact, easy to fabricate, integrate into the printed circuitry and is light weighted. The inclusion of metamaterial structures to the PIFA system makes it more compact, which will overcome the challenges faced in the miniaturization of antenna systems in mobile communication. This chapter gives an insight to the possibilities of designing a compact metamaterial PIFA system.

#### 2.1.1 PIFA System

The conventional PIFA is also known as quarter-wavelength patch antenna as it is resonating at quarter wavelength, i.e., at  $\lambda/4$ . Since the antenna is resonant at the quarter wavelength, the size of the antenna is less and hence occupying little space. PIFA systems have wide applications such as mobile hand sets. This chapter also provides a feasibility study of metamaterial PIFA system in the cellular bands. The frequency bands for cellular phone systems are as follows: GSM (Global System

---

S. Manjula · B. Choudhury (✉)

Centre for Electromagnetics, CSIR-National Aerospace Laboratories, Old Airport Road, Bengaluru 560017, India

e-mail: balamati@nal.res.in

© Springer Nature Singapore Pte Ltd. 2017

B. Choudhury (ed.), *Metamaterial Inspired Electromagnetic Applications*,

DOI 10.1007/978-981-10-3836-5\_2

for Mobile Communications: 880–960 MHz), DCS (digital communication system: 2.71–1.88 GHz), PCS (Personal Communication System: 1.85–1.99 GHz) and IMT-2000 (3G: 1.92–2.17 GHz).

### ***Advantages of PIFA System***

PIFA systems are chosen for its simple and compact structure. They can be easily installed in cellular devices. The main advantages of PIFA are mentioned below:

- The advances in printed circuit technology make antenna fabrication quite easier and cost-effective.
- As the size of the PIFA antenna is in the order of quarter wavelength, it found applications in UHF and VHF range.
- Enhanced antenna performance such as low SAR due to its reduced backward radiation.
- A single-patch PIFA system itself provides a maximum gain in the range of 6–9 dBi.
- The gain of the antenna can be enhanced by using an array of patches on a single substrate, which makes the antenna cost-effective as compared to other antennas.
- PIFA systems possess good electrical characteristics.
- It can be tuned easily, and impedance matching can be done by varying the position of the feed.
- It can be used for MIMO (multiple-input and multiple-output) applications.
- The losses of PIFA system are low as compared to other antennas.

### ***Limitations***

Planar inverted-F antenna is characterized by narrow bandwidth. The shorting pin known to reduce the size of the antenna will result in narrow impedance.

## ***2.1.2 Applications of PIFA System***

Planar inverted-F antenna finds applications in wireless applications such as cellular devices, biotelemetry communication, healthcare applications, WLAN and WIMAX applications for laptop. These applications require a much smaller antenna with a better performance and enhanced bandwidth.

*Biotelemetry application:* Recently, PIFA systems have been used in biotelemetry communication system for treatment of human diseases and also to monitor the signals within the human body. In biotelemetry systems, the antenna is implanted into the body. The body is continuously monitored by transmitting and receiving the physiological signals between implanted antenna and the medical communication device.

*Radio frequency identification:* Hospitals have advanced a lot in the recent years, by making use of the technologies available in the market to minimize medical errors and to provide better quality of healthcare in the hospitals. RFID tags which

make use of PIFA system comes in handy by providing security solutions, and locating and tracking hospital staff in case of emergencies which is efficient for the hospitals to deliver a prompt service. RFID collars are also developed using PIFA system. The collars are usually worn by the cattle in a large herd. In case of theft or any other danger, the cattle will start running. The acceleration is detected by the device, and a message is sent to farmer through GSM network, making it easy to find the cattle.

*WLAN/WIMAX applications:* PIFA offers many attractive features such as small structure, low cost and better performance. These features have made it attractive in the field of wireless technology. PIFA serves as wireless local area network antenna for the laptop computers. In the recent trends, it has become a standard element in laptops for wireless internet access, due to its small structure. PIFA system is also used in cellular devices to provide wireless LAN services.

### 2.1.3 Design Challenges

Although there are various techniques and different simulation tools, the following issues make the design of PIFA system a truly challenging aspect.

*Downsizing the antenna:* The size of the antenna cannot be decreased just by scaling or by reducing the dimensions of the antenna since the impedance at antenna's terminals will be affected. The other factors which will be affected by reducing the size of the antenna are its radiation characteristics. Also, the gain, bandwidth and efficiency will be greatly influenced. The other limitation in reducing the size of the antenna is the difficulty in feeding small antennas correctly. Small antennas are greatly affected by their surroundings, so care should be taken to integrate such antennas into a system so as to obtain the maximum efficiency. Hence, we can say that reducing the size of antenna is to compromise the best bandwidth and efficiency among the obtained set of values. The other issues in design of antenna are discussed below.

*Integrating with other components:* While integrating an antenna onto the board of the mobile phones, the neighboring components has to be taken into consideration since they influence the performance of antenna greatly. With the advancement of multimedia components in cellular devices, the space for antenna started shrinking and antenna had to be integrated with other components. The cellular device consists of battery, display, speakers, camera and other components. These components act as noise source to the antenna since they emit RF noise which will degrade the performance of the antenna. Hence, care should be taken while integrating these components with the antenna so as to minimize its effect on the antenna performance and obtain maximum output performance.

*Mechanical issues:* Once the antenna is being designed electrically, the next step is to provide a mechanical solution to the electrical design. To maintain the efficiency of the antenna, it is necessary to have good mechanical contact and

tolerance. Also, the distance between metal objects and lossy objects needs to be optimized for the better performance.

*Quality issues:* An antenna is quality-controlled through its design. To have a better quality, the antenna needs to be simple with few contact points. The distance between feeding pins and the ground pins needs to be large to improve tolerance.

*Connection issues:* Connection is another issue which needs to be considered to maintain the quality of the antenna. The antenna suffers ohmic losses due to the number of connections. This can be reduced by having direct connections to the PCB as much as possible.

## 2.2 Reviews on PIFA

A brief description about planar inverted-F antenna is given in this section. The concept of miniaturization, need for it and the challenges faced in miniaturization are discussed. Different techniques on miniaturization of the antenna are studied, and review is provided towards enhancing the gain of the antenna. Based on the survey, suitable technique for miniaturization is opted and is used in our design.

### 2.2.1 Basic PIFA System

Planar inverted-F antenna gets its name from its shape which is in the form of an inverted F. Figure 2.1 shows the schematic of a basic PIFA antenna consisting of a ground plane, substrate, feeding pin and a radiating patch shorted at one end through a shorting pin. The radiating patch is placed above the ground plane so as to be parallel with it. This in turn introduces capacitance to the input impedance of the PIFA system which is compensated by adding a short-circuit stub. When the PIFA

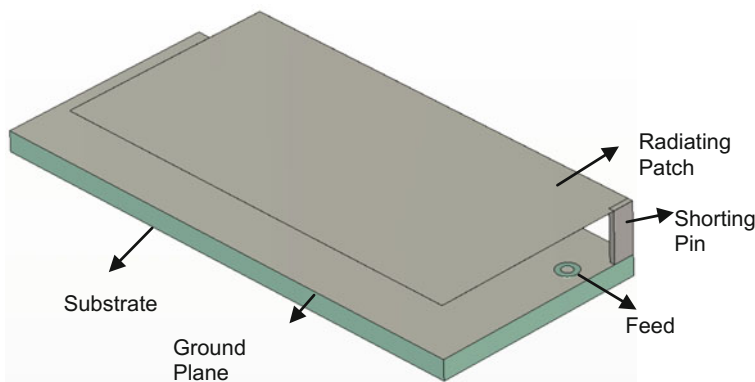


**Fig. 2.1** Schematic of a conventional PIFA system

is excited, currents in the ground plane are also excited, which forms an electromagnetic field. The ground plane and the antenna combination acts as a perfect reflector only when the dimensions of the ground plane are larger than the antenna, i.e., the ground plane length required is  $\lambda/4$ , where  $\lambda$  is the operating wavelength. If the length of the ground plane is below  $\lambda/4$ , then the antenna possesses problems for the tuning mechanism, thereby reducing antenna's performance, while multi-lobes are introduced if the length of the ground plane is greater than  $\lambda/4$ . The feeding pin is placed in between the open end and the shorter end of the patch.

The input impedance of the PIFA can be controlled by varying the position of the feed. The impedance of the PIFA decreases when the feed is closer to the shorting pin, while the impedance increases when the feeding pin is moved away from the shorting pin. The impedance of PIFA can be tuned using this parameter. The resonant frequency of the PIFA system is dependent on the width "D" of the shorting wall. If the width of the patch is equal to the width of the shorting wall, then the shorting pin runs the entire width of the patch. The antenna has maximum radiation efficiency when

$$L = \lambda/4 \quad (2.1)$$

If the width of the short is zero, then the antenna resonates at

$$L + W = \lambda/4 \quad (2.2)$$

From the above two equations, it is seen that the antenna resonates when the space between the edge and the shorting area is a quarter wavelength. The resonant length of the antenna is approximated as

$$L + W - D = \lambda/4 \quad (2.3)$$

### 2.2.2 Miniaturization of PIFA

In these days, the size of the antenna in cellular phones is a major concern, as the space available for antenna in mobile phone is reducing. Hence, we primarily focused on reducing the size of the antenna while improving the gain of antenna with low SAR. Different techniques have been investigated for miniaturization of PIFA system and are given below.

#### *Capacitive loading technique*

Capacitive loading is the most common technique used to reduce the size of the conventional PIFA system. In this technique, capacitance is introduced between the open edge and feeding point as shown in Fig. 2.2. Such antennas are known as lumped element-loaded antennas.

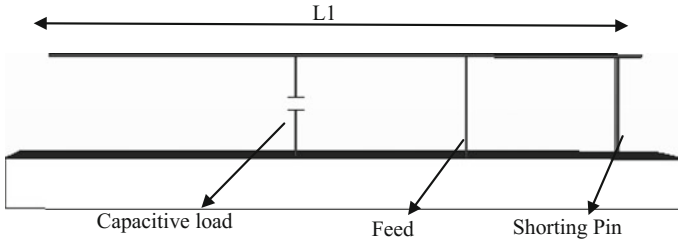


**Fig. 2.2** Capacitive-loaded antenna

Chi et al. [1] proposed a miniaturized PIFA system by loading lumped elements achieved from transmission line model. The electrical size of the antenna is reduced to one-eleventh (reduction by 91%) after loading shunt capacitors periodically. The experimental results show that although the size is reduced significantly, the measured radiation gain and bandwidth are reduced to  $-22.6$  dBi and 0.15%, respectively.

#### ***Magnetic material loading technique***

Loading the antenna with magnetic materials is another known technique to reduce the size of the antenna. Kawano et al. [2] designed PIFA systems by loading magnetic materials in the feed and the shorting pin of the PIFA system. The corresponding input impedance, surface current distribution and the radiation characteristics of the antenna were obtained and compared with the calculated results. It is seen that the PIFA loaded with magnetic materials was 50% smaller in structure than the PIFA without magnetic materials.

Karkkainen et al. [3] used magnetic material fillings to reduce the size of the PIFA system. The PIFA system is designed using the dispersive magnetic material fillings between the ground plane and the radiating patch. The designed PIFA is simulated using FDTD method, and the effect of resonant frequency of the materials on the resonant frequency of the PIFA is studied. It has been observed that the resonance frequency of the PIFA is reduced by 20% due to the resonant magnetic material, while the relative bandwidth is retained.

#### ***Metamaterial-based PIFA system***

In the recent years, metamaterials have inspired great deal of interest due to their unique properties such as negative permittivity and negative permeability. Metamaterials are not readily available in nature, and these materials are artificially engineered to obtain the negative characteristics by periodically arranging thin-wire structures. Split ring resonators on the other hand are also known to exhibit negative refractive index.

Xin-Yuan et al. [4] proposed a novel design of metamaterial-loaded wideband PIFA system. An array of Jerusalem cross-shaped PEC structure used in frequency-selective surface (FSS) is designed, which acts as a metamaterial structure. This metamaterial structure is loaded on the ground plane of the PIFA

antenna. In metamaterial-loaded PIFA system, the size was reduced by 91%. The center frequency of the PIFA system is found to be 3.4 GHz.

### ***EBG-based PIFA systems***

The growing interest in electromagnetic band gap (EBG) structures paved way for researchers to utilize them in miniaturization of antenna. EBG structure helps in reducing surface waves, thereby enhancing the bandwidth, forward and backward radiation ratio, directivity and efficiency of the antenna.

Zuazola et al. [5] proposed a miniaturized PIFA system using FSS strips which act as EBG structures. FSS strips are incorporated on the bottom layer of the PIFA system to increase the bandwidth and front-to-back ratio. The frequency of operation of the FSS-based PIFA system was 1–6 GHz. PIFA with FSS strips mounted on a FR4 substrate having extra ground plane can broaden the bandwidth and is suitable for GSM 900 band. The miniaturized multiband PIFA with FSS strips can work satisfactorily at the DCS-1800, UMTS, Hiper LAN/2 bands and Bluetooth (WLAN).

Zhao et al. (2004) [6] proposed an EBG-based PIFA system to downsize the PIFA system. The designed antenna consisted of mushroom-like EBG structure operating from 2.1 to 2.4 GHz having metallic patches, connecting pins, a ground plane and a dielectric substrate. From the simulated results, it was seen that the PIFA with EBG had a reduced thickness of 2.6 mm as compared to the conventional PIFA.

## ***2.2.3 Performance Enhancement of PIFA***

Since years, there have been growing demands in the market for smaller antennas that can be easily embedded in cellular devices. This calls for the attention toward enhancing the performance of the antenna. Several researchers have been trying to find different methods to improve the performance of the antenna. Different techniques are discussed here to enhance the performance of the antenna.

### ***Using electronic band gaps***

EBG structures stand out as an option because of its unique properties and characteristics such as surface wave suppression and in-phase reflection coefficient. The surface wave suppression characteristic is often utilized to enhance the gain of the antenna and to reduce the mutual coupling, while the latter can be utilized to design low-profile antennas. EBG as metamaterials are used to control the propagation of waves at all incident angles and polarizations. EBG are also known as photonic crystals and are realized using periodic arrangement of metallic structures.

Zhao et al. (2004) [6] designed an EBG-based planar inverted-F antenna to increase the efficiency of the antenna. Mushroom-like EBG structure operating from 2.1 to 2.4 GHz having metallic patches, connecting pins, a ground plane and a dielectric substrate was used. EBG structures are capable of controlling the flow of electromagnetic waves. Compared to the conventional PIFA, PIFA with EBG

structure has 6 dB reductions in backward radiation. The resonant frequency is shifted from 2.7 to 2.4 GHz.

EBG structure reduces surface waves, thus leading to an increase in directivity, bandwidth, forward and backward radiation ratios, and efficiency.

Abidin et al. [7] proposed a  $2 \times 2$  U-shaped PIFA system at 2.4 GHz and reduced the mutual coupling effect using EBG structures. The designed antenna had a thin profile and was fabricated in FR4 substrate, which can be useful in compact mobile handsets. The EBG-based PIFA system reduced the mutual coupling by 6 dB.

### *Using metamaterials*

Attia et al. [8] used metamaterials as superstrate to enhance the gain of a PIFA system working at UMTS band. Split ring resonators with high value of permeability at resonant frequency of the antenna were used as superstrate. A  $12 \times 12$  array of metamaterial SRRs was used as superstrate on a conventional planar inverted-F antenna, which increased the antenna gain by 3.2 dB.

Xin-Yuan et al. [4] designed a metamaterial-loaded wideband PIFA antenna using frequency-selective surfaces (FSS). The FSS consisted of an array of Jerusalem cross-shaped PEC structure which acts as a metamaterial structure. This metamaterial structure is loaded on the ground plane of the PIFA system. The metamaterial-loaded PIFA system has an enhanced bandwidth of 49.4% from 2.56 to 4.24 GHz at a center frequency of 3.4 GHz.

To summarize, metamaterials play an important role in miniaturization and performance enhancement of PIFA system. The antenna size can be reduced significantly using metamaterial split ring resonators, metamaterial EBG structures and Jerusalem cross designs in the ground plane, to act as metamaterial. Hence, the literature survey reveals that metamaterial structure helps in miniaturization as well as performance enhancement of PIFA system.

## **2.3 Background Theories for the Design of PIFA System**

This section provides an overview of the concepts used in design of PIFA system. As per our approach toward miniaturization, a basic PIFA system will be designed and the corresponding results for the designed antenna structure shall be obtained. The theory of metamaterials has been discussed, and a suitable metamaterial structure is selected for PIFA design. The selected metamaterial structure will be then optimized for desired resonant frequency. The designed metamaterial is loaded onto the basic antenna as per the proposed design, and the results are obtained. Further optimization of the novel PIFA has been carried out in order to achieve high system performance. The designed antenna with metamaterials is then compared with the results of the basic antenna structure, and its performance characteristics are studied.



### 2.3.1 Metamaterial Structure

From the literature survey, it could be seen that the metamaterial structure improves the performance of the PIFA system and also helps in downsizing the antenna. The most popular kind of metamaterial structure is the SRR. A single SRR can be modeled as an LC circuit. Figure 2.3 shows a simple square SRR. The SRR in the figure consists of a coil which forms an inductor, while the open ends of the coil form the capacitor.

The gaps between the rings are considered for the prediction of resonant frequency. Since the SRRs exhibit negative permeability close to their resonant frequency, it is important to predict the proper resonant frequency for a chosen structure.

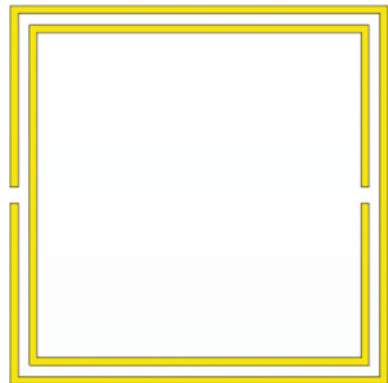
#### Design of SRR

A split ring resonator is the most common structure used to obtain negative refractive index in designing metamaterials. SRRs were obtained initially from the wire structure by Sir Pendry [9]. SRRs can produce magnetic resonance leading to negative permeability. The return loss of antenna is tuned by magnetic resonance of the SRR which results in the improvement in size of the antenna. Further, the interaction between magnetic field of SRR and the fields generated by PIFA system will enhance the radiation properties, return loss, bandwidth and gain of antenna. The SRR structure considered here consists of two concentric square rings. Each ring has a gap appearing on opposite sides. Schematic of a simple square split ring resonator is shown in Fig. 2.3. In order to isolate the inclusions and their electric and magnetic properties, the non-planar concept was employed. The relative negative permittivity and permeability are given by

$$\varepsilon_r = n/\eta \quad (2.4)$$

$$\mu_r = n\eta \quad (2.5)$$

**Fig. 2.3** A simple square split ring resonator



### 2.3.2 Specific Absorption Rate

The rate at which radiation is absorbed by the human body is measured by the specific absorption rate (SAR). It is usually measured over 1 gm/10 gm of human tissue. SAR is defined as

$$\text{SAR} = \frac{\sigma E^2}{\rho} (\text{W/kg}) \quad (2.6)$$

where  $E$  is the root-mean-square amplitude of induced field,  $\sigma$  is the conductivity of tissue, and  $\rho$  is the mass density of tissue. The radiation emitted from cellular devices is regarded as the top polluting sources by World Health Organization which may lead to health hazards in humans. Different countries around the globe have specified different standards to limit SAR produced from cellular devices. In USA, the specified SAR value is below 1.6 W/kg over 1 gm of tissue, while in Europe, the specified limit is around 2 W/kg over a tissue volume of 10 gm. India has adopted FCC standards to limit SAR. The value of SAR depends on volume of the head that has been exposed to radiation and also the position of cellular device to the head. For mobile applications, in order to reduce the electromagnetic interaction between human head and mobile phone, SAR has to be controlled. Various methods have been proposed towards reduction of SAR in human head.

Lin et al. [10] designed a FSS-based PIFA system towards reduction of SAR. The SAR was reduced by decreasing the backward radiation using two-dimensional periodic structure of frequency-selective surface (FSS) structure which was placed at the bottom side of the PIFA system. The resonating frequencies of the designed antenna are at 900 and 1800 MHz. The integration of PIFA and FSS also improves the antenna gain and radiation efficiency of the antenna. The total dimension of the PIFA system was reduced after addition of slotted FSS structure.

Manapati et al. [11] used metamaterial split resonators to reduce SAR of PIFA system. They proposed three different types of resonator such as spiral resonator (SR), split ring resonator (SRR) and open split ring resonator (OSRR) as metamaterial unit cell. The array of resonators exhibits negative permeability. The PIFA system which was resonating at 900 MHz was tilted by 30°, and the face of the antenna is in the direction opposite to the human head. By using the 10-element array of spiral resonator, split ring resonator and open split ring resonator, the SAR has been reduced by 35.52, 20.12 and 57.89%, respectively.

Faruque et al. [12] carried out electromagnetic absorption studies in mobile phones while using metamaterials in the antenna system. An array of metamaterials is kept in between the antenna and human head to reduce the SAR. A finite-difference time-domain (FDTD) method with lossy-Drude model was used for this analysis. In order to study the reduction in SAR, various parameters have been investigated, such as the effects of attaching the metamaterial at different positions, distance and size of metamaterials, perfect electric conductor and

materials on the specific absorption rate reduction. The PIFA is constructed with helical-type antenna, which is resonating at 900 MHz, and is used for GSM applications. The metamaterial characteristics were obtained by arranging the split ring resonators periodically. The structure exhibits metamaterial properties at 900 and 1800 MHz. These metamaterial structures are designed on a printed circuit board for the easy integration with cell phones. Metamaterials helped to achieve a 42.12% reduction of the initial specific absorption rate value for 1 gm specific absorption rate and 53.94% reduction for the 10 gm specific absorption rate. Further, Faruque et al. [13] proposed a new design of square metamaterial structure and used as an array of metamaterials to reduce the absorption rate. The design was experimentally validated.

### 2.3.3 Optimization of PIFA Using PSO

The proposed PIFA system is designed using square SRR as metamaterials. The design of PIFA system involves varying the position of feed and changing the dimensions of shorting wall and radiating patch for better performance, and also the metamaterial needs to be designed to match the resonant frequency of the PIFA system which is a time-consuming task. Hence, optimization is done to obtain the required parameters for a good design. This calls for the implementation of different optimization techniques.

Soft computing technique stands as an option among various techniques due to their properties such as global optimization, quick response and accuracy. The emerging trends in soft computing techniques play an important role in the optimization of the design in various fields of electromagnetics including metamaterials. These techniques yield quick and robust solutions that are economically viable. Soft computing techniques have been earlier used to optimize the design of antennas and metamaterials.

Here, a square SRR as metamaterial in conjunction with PIFA system is used to downsize the antenna in order to enhance the performance of it. To accomplish this, an array of square SRRs is loaded on the antenna by replacing the ground plane. The SRR array needs to be designed at a frequency range which is equivalent to the resonant frequency of the PIFA system. To design the SRR at a particular resonant frequency, particle swarm optimization (PSO) is developed.

## 2.4 Design Methodology

PIFA systems are widely used in wireless communications due to their compactness and multiple-input and multiple-output applications. However, these antennas possess a narrow bandwidth which is a disadvantage and also the size of the antenna is to be taken into consideration. In order to increase the performance of the

antenna and also to reduce its size, a simple square ring resonator is proposed along with conventional PIFA. The square ring resonator is to be designed at a resonant frequency equivalent to the resonant frequency of the PIFA system. PSO algorithm is used to optimize the structural parameters of the SRR for the desired resonant frequency. The optimized design of SRR is used in miniaturization of the antenna and to enhance the performance. The steps below are followed to design PIFA system.

- Step 1: Design of a conventional planar inverted-F antenna using transmission line model (for the required resonant frequency).
- Step 2: Selection of metamaterial structures and development of equivalent circuit model.
- Step 3: Optimization of the selected metamaterial structures for the desired resonant frequency using particle swarm optimization (CAD package developed by CEM, CSIR-NAL).
- Step 4: Design and simulation of optimized metamaterial structures. Using these metamaterial configurations, the PIFA system will be designed. The implementation of metamaterial structures as substrate or superstrate or hybrid ground plane depends on the EM requirements and application.
- Step 5: To achieve high performance, optimization of the metamaterial PIFA system will be carried out using soft computing techniques.
- Step 6: A comparative study of performance parameters of conventional PIFA system with metamaterial PIFA system will be carried out.

#### 2.4.1 Design of a Conventional PIFA System in C-Band

The aim of this work is to downsize the PIFA system using metamaterials. As the first step, we design the basic PIFA system by interfacing FEM-based electromagnetic solvers with MATLAB and study its characteristics so as to compare its results with the metamaterial-loaded antenna. The structure of the conventional PIFA is shown in Fig. 2.4.

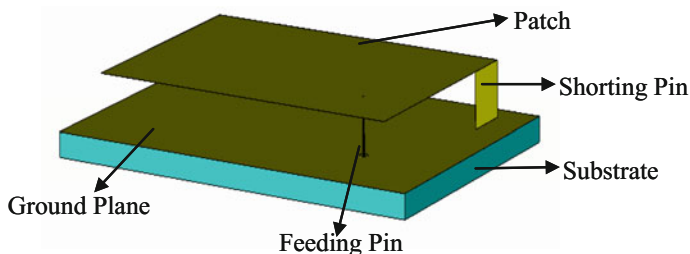


**Fig. 2.4** Structure of PIFA without metamaterials

It consists of a ground plane, radiating patch, substrate, shorting pin and a feeding pin. The substrate has a dielectric constant of 2.55. Copper material is used for the radiating patch, shorting pin, feed and the ground plane. The proposed metamaterial-loaded antenna design is shown in Fig. 2.5. The return loss characteristics are shown in Fig. 2.6. Also Figs. 2.7, 2.8 and 2.9 demonstrate the radiation characteristics obtained for the conventional PIFA system. Figure 2.10 shows the graphical user interface for the design of metamaterial SRR and Table 2.1 provides the design parameters for the PIFA system.

The frequency sweep is set from 1 to 8 GHz. The center frequency is taken at minimum return loss, and the bandwidth can be calculated from return loss

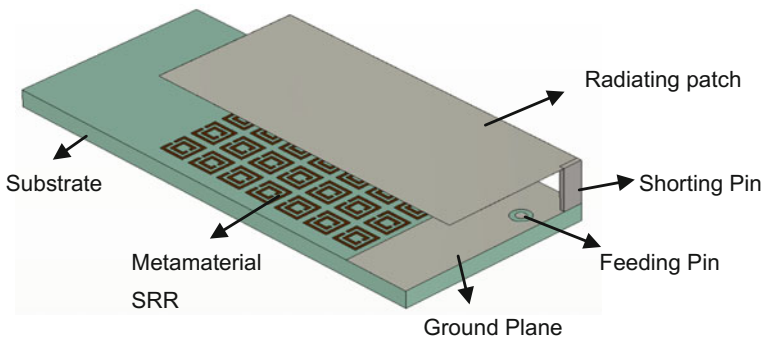


**Fig. 2.5** Structure of proposed PIFA design with metamaterial

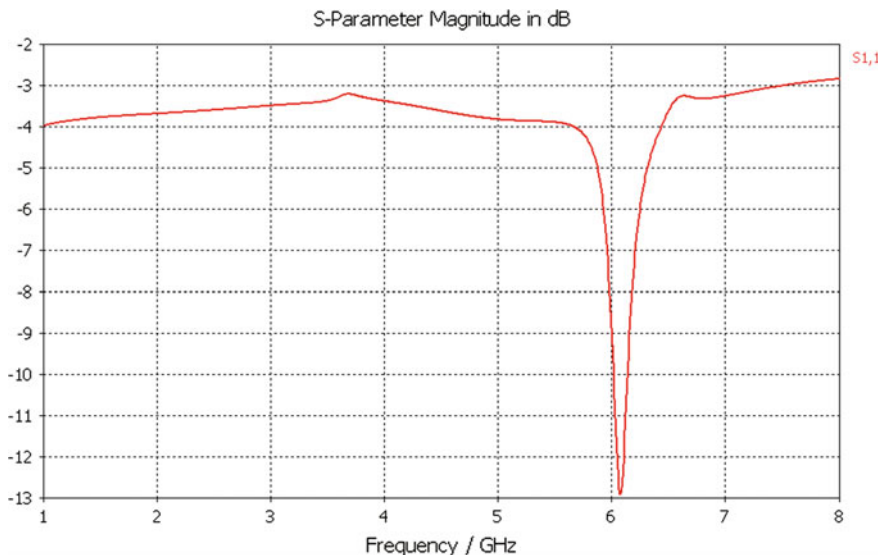


**Fig. 2.6** Return loss characteristics of conventional PIFA structure

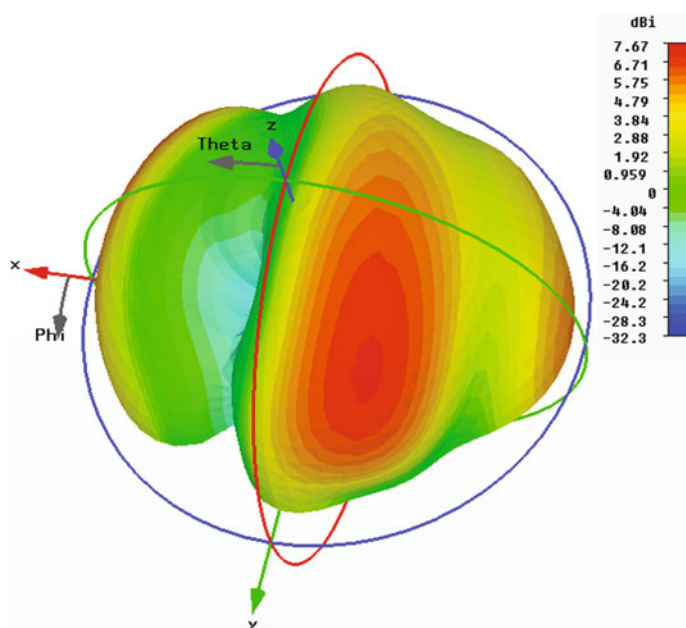


**Fig. 2.7** Radiation pattern of the conventional PIFA structure

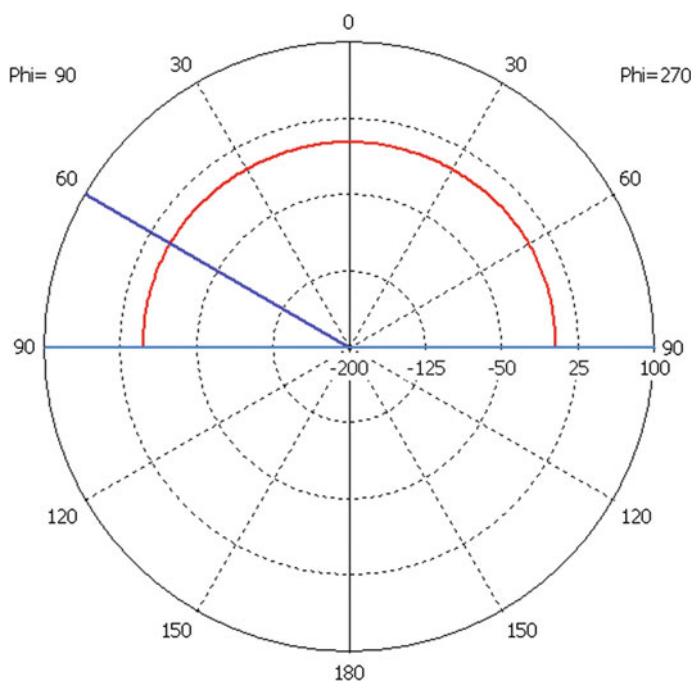


**Fig. 2.8** Impedance plot ( $\phi = 90$ ) of conventional PIFA structure

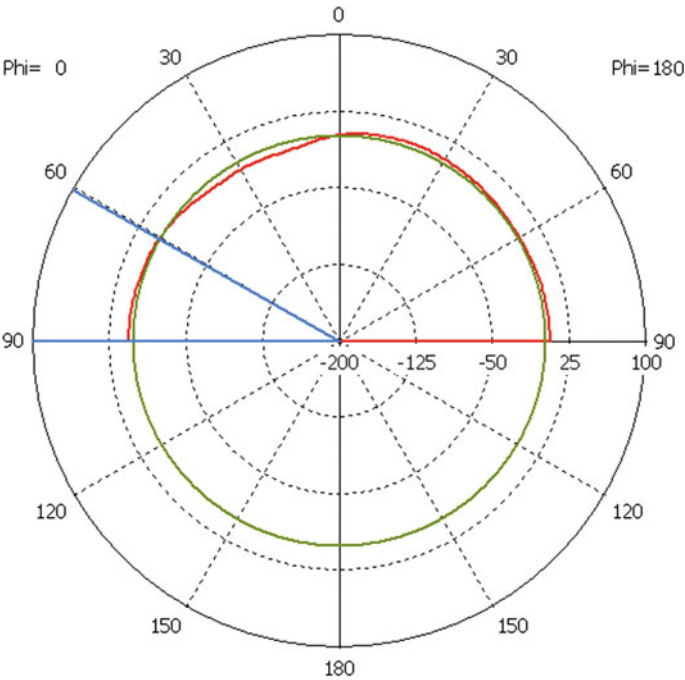


Fig. 2.9 Polar plot (phi = 0) of the conventional PIFA structure

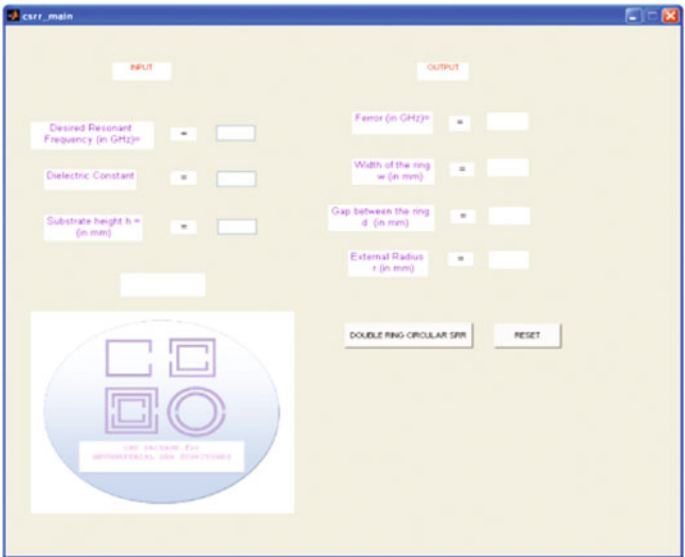


Fig. 2.10 Graphical user interface of PSO-based CAD package for design of metamaterial structures

**Table 2.1** Dimensions of conventional PIFA system

Parameter	Value (mm)
Width of the substrate, $W$	25
Length of the substrate, $L$	40
Distance of the feed in $x$ -axis, $f_x$	5.5
Distance of feed in $y$ -axis, $f_y$	5.6
Width of the radiating patch, $W_r$	20
Length of the radiating patch, $L_r$	32
Height of the patch from ground, $h$	3.5
Thickness of the substrate, $T$	2

**Table 2.2** Performance parameters of conventional PIFA system

Frequency	6.075 GHz
$S_{11}$	-12.893 dB
Gain	3.474 dB
Directivity	7.670 dBi

characteristics. The bandwidth of the antenna is taken for the frequencies above which the return loss is more than 10 dB. For the designed dimensions, the antenna is resonating at 6.075 GHz with return loss of 12.893 dB. The bandwidth of the antenna is found to be 23.28 MHz with center frequency of 6.075 GHz. The obtained antenna performances are shown in Table 2.2.

## 2.4.2 Design of Metamaterials

Square split ring resonators are the variant of split ring resonators used commonly in the design of metamaterials. It consists of two square-shaped rings with each ring consisting of a gap. The rings are placed in such a way that the gap on one ring is opposite to the gap on the other ring. Square SRR at 6 GHz is chosen as metamaterial unit cell. The frequency of SRR is designed to match the frequency of PIFA system.

### *Design of square split ring resonator*

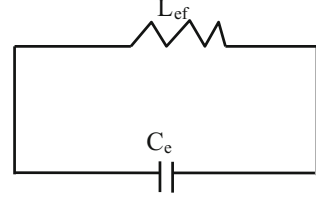
The design starts with a single SRR unit cell initially, and further, the SRR array is used according to the antenna size. For the preliminary design, structural dimensions of SRR structure are obtained using PSO-based CAD tool. The GUI window of the CAD tool is shown in Fig. 2.10. The CAD tool is capable of designing the SRR structure at any resonant frequency which is a priori requirement in metamaterial-based PIFA system. The dimensions calculated from the CAD tool are then optimized to obtain the desired resonant frequency.

### *Equivalent circuit model of square split ring resonator*

The square SRR can be modeled as LC parallel tank circuit. The gap in the ring forms the capacitor, while the metal ring forms the inductor. The values of capacitance and inductance of the split ring resonators are determined using the



**Fig. 2.11** Equivalent circuit of square split ring resonator



equivalent circuit shown in Fig. 2.11. From the equivalent circuit analysis, resonant frequency of the SRR is given by

$$w_0 = \frac{1}{2\pi\sqrt{L_{ts}C_{eqs}}} \quad (2.7)$$

where  $C_{eqs}$  is the total equivalent capacitance and  $L_{ts}$  is the total effective inductance of the SRR.

The total equivalent capacitance is given by

$$C_{eqs} = \left(a - \frac{3}{2}(w + d)\right) C_{pul} \quad (2.8)$$

where  $C_{pul}$  is the per-unit-length capacitance between the rings.

$$C_{pul} = \epsilon_0 \epsilon_{eff} \frac{K(\sqrt{1 - k^2})}{K(k)} \quad (2.9)$$

and  $\epsilon_{eff}$  is the effective dielectric constant given by

$$\epsilon_{eff} = \frac{\epsilon_r + 1}{2} \quad (2.10)$$

$K(k)$  denotes the complete elliptical integral of the first kind with  $k$  denoted as

$$k = \frac{d}{d + 2w} \quad (2.11)$$

The total effective inductance of the square SRR is given by

$$L_{ts} = \frac{4.86\mu_0}{2}(a - w - d) \left[ \ln\left(\frac{0.98}{\rho}\right) + 1.84\rho \right] \quad (2.12)$$

where  $\rho$  is the filling factor given by

$$\rho = \frac{w + d}{a - w - d} \quad (2.13)$$

**Fig. 2.12** Optimized design of square SRR

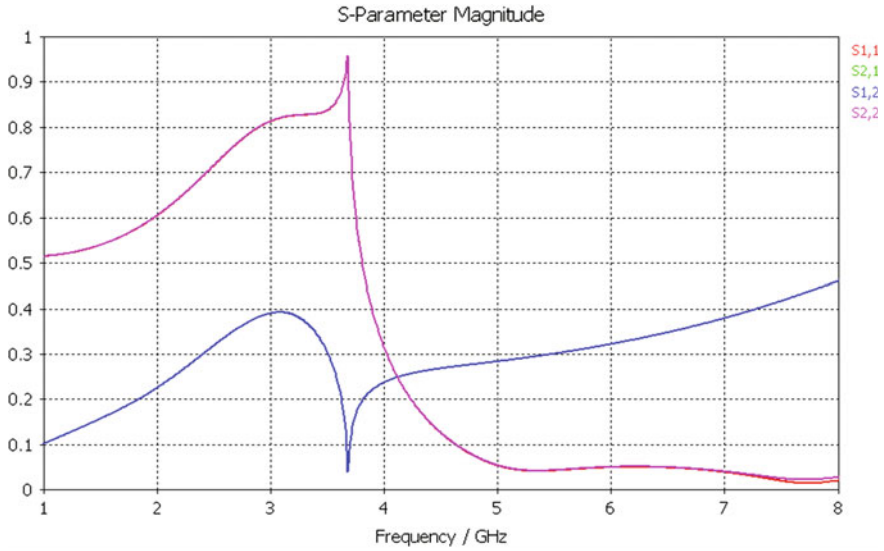
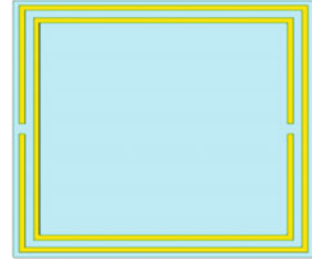


**Fig. 2.13** Scattering parameters of square SRR

### ***Simulation of square split ring resonator***

Numerical simulations are used to predict the transmission properties of SRRs. Here FEM-based solver is used to simulate the SRR structure. The simulations are done by propagating EM wave along Y-direction. Z-axis was electrically polarized, and X-axis was magnetically polarized. The background material was assumed to be vacuum. To validate the simulation, the SRR parameters were chosen to be  $d = 0.1204$  mm,  $g = 0.2408$  mm,  $c = 0.6995$  mm and  $l = 5.2$  mm. The thickness and dielectric constant of the substrate were 2 and 2.55 mm, respectively. Table 2.3 provides the structural parameters of the metamaterial unit cell. The structure was then optimized for resonant frequency of 6 GHz, and the corresponding permittivity and permeability were extracted. Figure 2.12 shows the optimized structure of square SRR, and the simulation results are shown in Figs. 2.13, 2.14 and 2.15. From the simulation results, it has been observed that the designed square SRR metamaterial has negative material characteristics from 4 to 6 GHz.

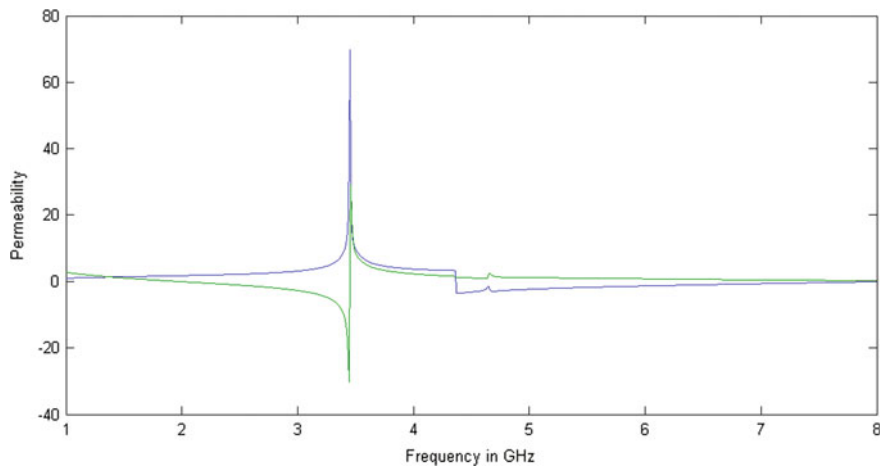


Fig. 2.14 Extracted permittivity of square SRR

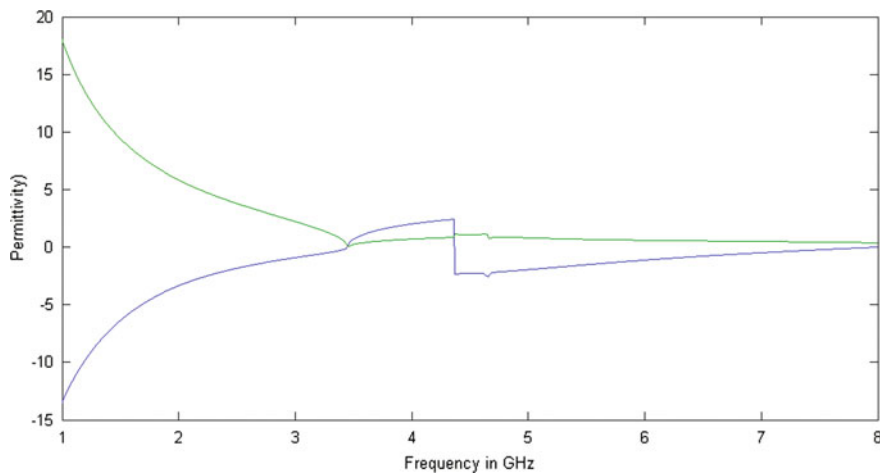


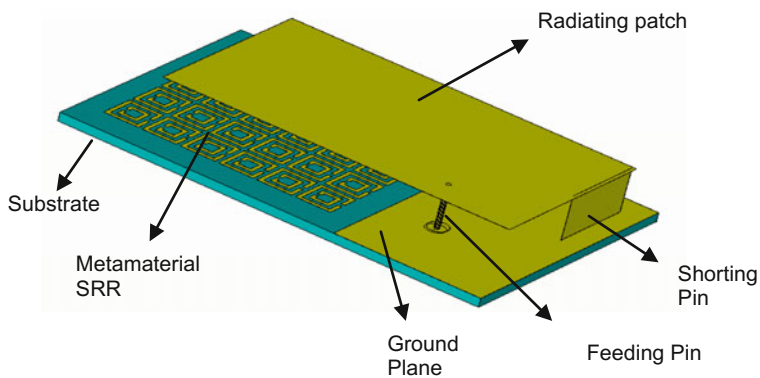
Fig. 2.15 Extracted permeability of square SRR

Table 2.3 Dimensions of designed metamaterial

Parameter	Value (mm)
Thickness of the substrate, $h$	2
Metal thickness, $t$	0.01
Width of the rings, $w$	0.6995
Length of outer ring, $o$	5.2
Gap in each ring, $g$	0.2408
Gap between rings, $d$	0.1204

### 2.4.3 Design of PIFA Antenna Using SRR

The design of PIFA with metamaterials is shown in Fig. 2.16. An array of SRRs is taken and placed on the substrate by replacing the ground plane. The antenna is then scaled accordingly to resonate at 6 GHz frequency. The design optimization and simulations are done by interfacing FEM-based EM solver with MATLAB. The structural dimensions of PIFA system using SRR has been optimized for better performance using soft computing based optimization algorithm in conjunction with EM solvers. The enhanced antenna characteristics are shown in Figs. 2.17, 2.18, 2.19, 2.20 and 2.21.



**Fig. 2.16** Structure of PIFA design with metamaterials

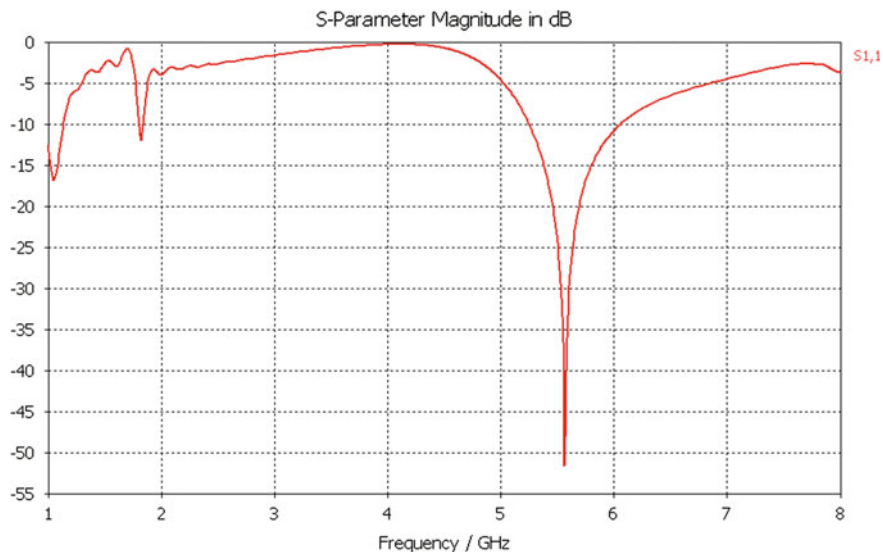


**Fig. 2.17** Return loss characteristics of PIFA system with metamaterials

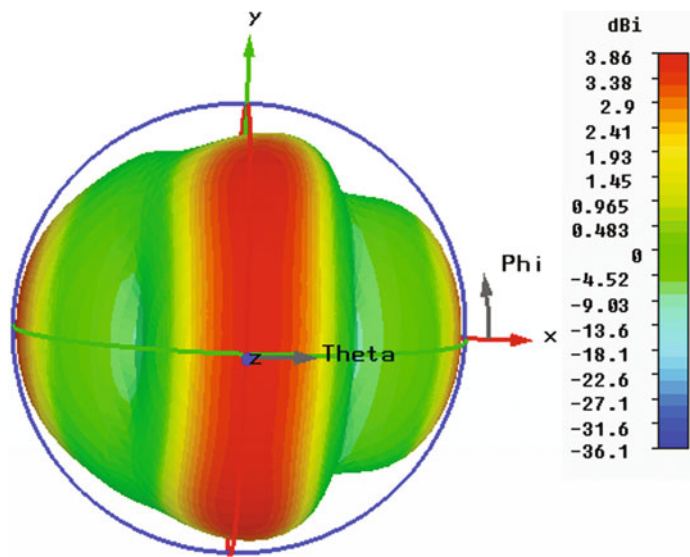


Fig. 2.18 3-D radiation pattern (directivity) of PIFA system

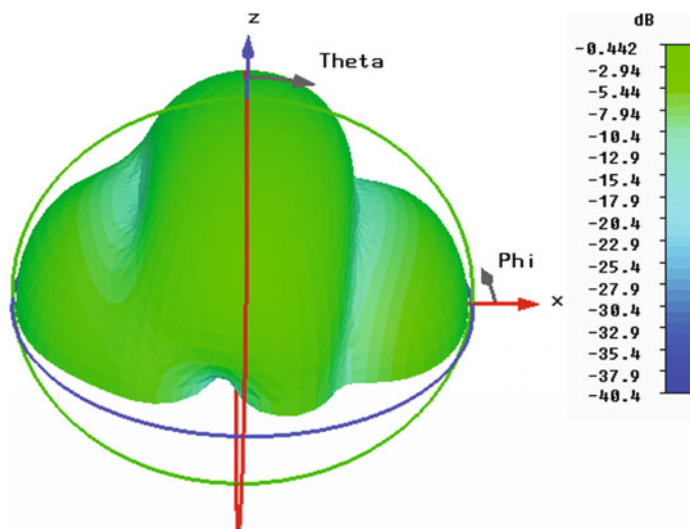


Fig. 2.19 3-D radiation pattern (gain) of PIFA system

The designed PIFA system with metamaterials resonates at a frequency of 5.564 GHz with return loss of 51.57 dB. The directivity at resonant frequency is 3.86 dBi. Table 2.4 provides the obtained antenna characteristics. From the results, it is clear that the return loss, gain and directivity of the metamaterial-loaded PIFA

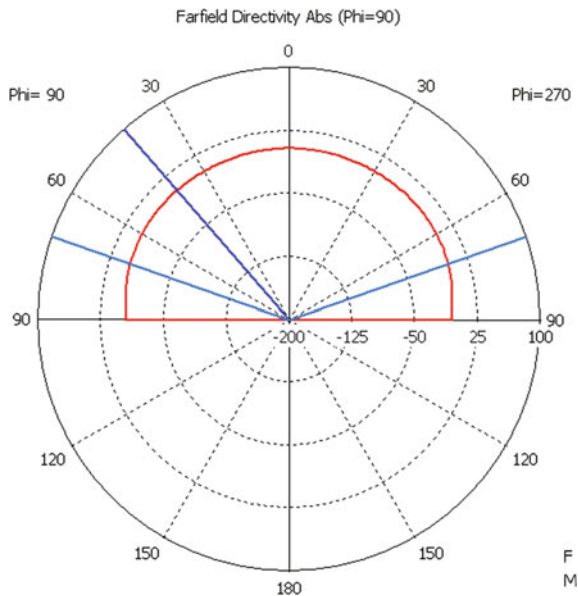


Fig. 2.20 Polar plot ( $\phi = 90^\circ$ ) of PIFA system

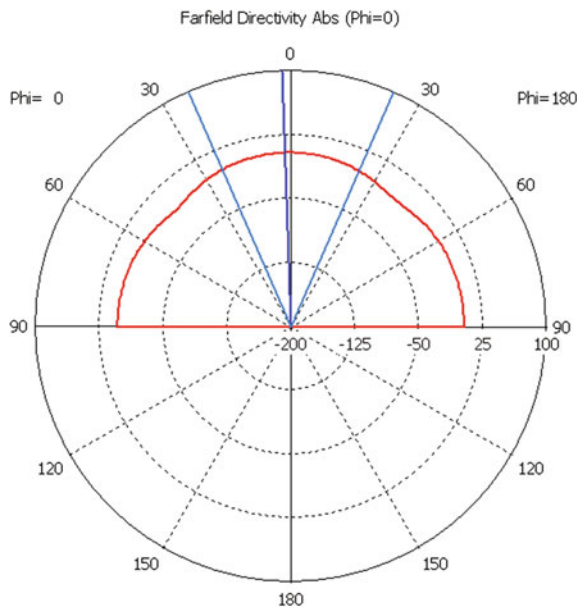
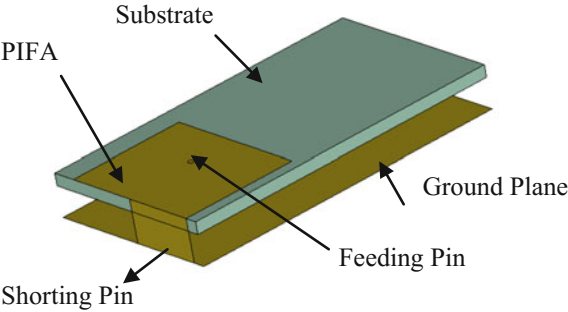


Fig. 2.21 Polar plot ( $\phi = 0^\circ$ ) of PIFA system

**Table 2.4** Performance parameters of metamaterial-based PIFA system

Frequency	5.564 GHz
$S_{11}$	-51.57 dB
Directivity	3.86 dBi

**Fig. 2.22** Schematic of a conventional PIFA system



antenna have been improved as compared to a conventional PIFA system without metamaterial inclusion.

**2.4.4 Design of PIFA Antenna Using PBG Substrate in S-Band**

The efficient antenna system can be achieved by enhancing bandwidth and downsizing the system. The PIFA with PBG structure will give admirable results compared to the conventional PIFA. In recent times, the PBG structure has been developed rapidly. The operation of the PBG mainly depends on periodicity, pattern, dielectric contrast and repetitive spacing between atoms. These structures do not let the propagation of electromagnetic waves for certain space directions in a given frequency range, which is very constructive feature. In this section, a novel PBG planar inverted-F antenna (PIFA) for wearable systems is presented.

The structure of the conventional PIFA is shown in Fig. 2.22. It consists of a patch, ground plane, shorting wall, feeding point and Teflon substrate. The thickness of the substrate is 2 mm with permittivity  $\epsilon_r = 2.1$ . The PIFA patch is manufactured on Teflon substrate. The shorting wall having length 25 mm and width 24 mm is placed to achieve the impedance matching. There is an air gap between substrate and ground plane, it will not change the field of antenna, but it can change the resonant frequency. The height of air gap is 6 mm. Copper material is used for radiating patch, shorting pin, feed and ground plane. The FEM-based solver is used to simulate the PIFA system. The detailed dimensions of conventional PIFA are given in Table 2.5, and the simulation results are shown in Figs. 2.23, 2.24, 2.25, 2.26.

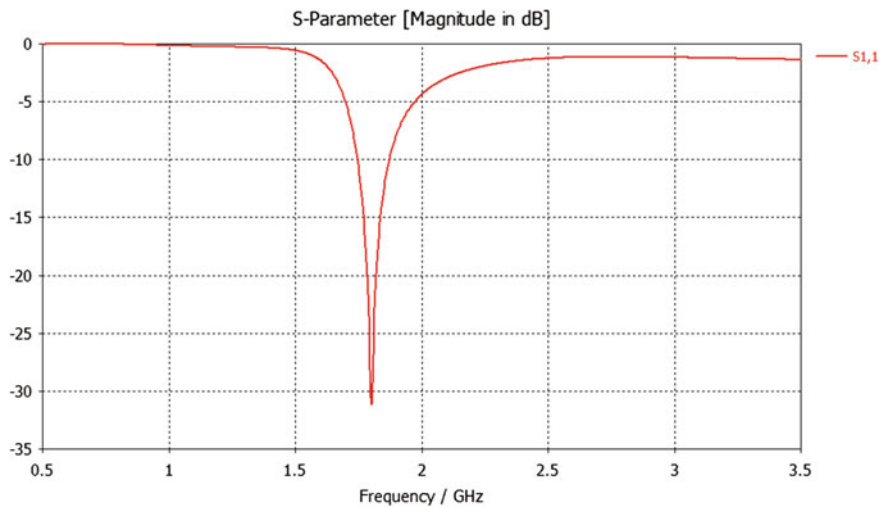


Fig. 2.23 Return loss (S11) for the conventional PIFA structure

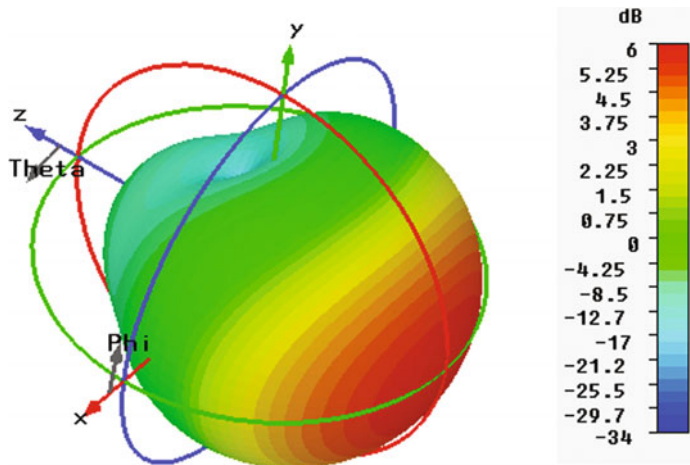
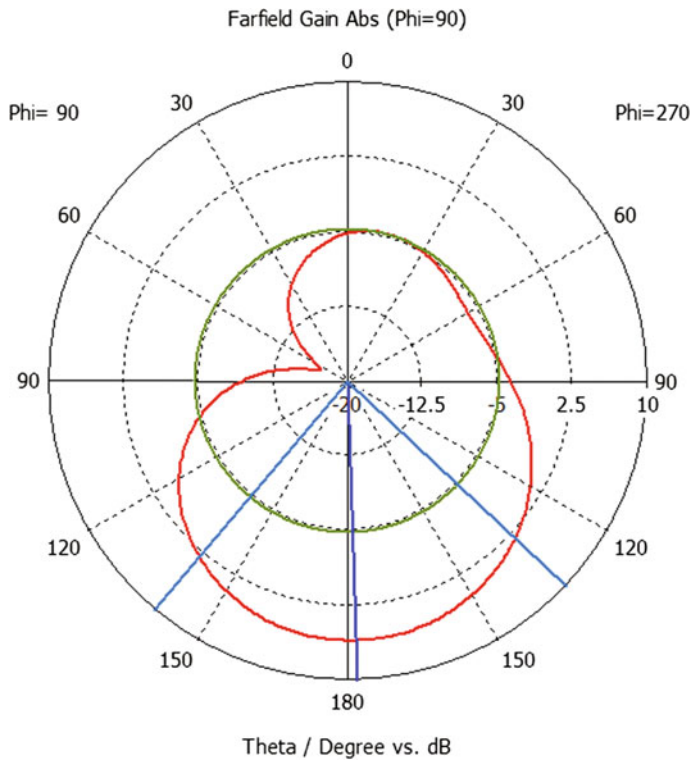


Fig. 2.24 Radiation pattern of the conventional PIFA structure

The frequency sweep is set from 0.5 to 3 GHz. For the designed dimensions, the antenna is resonating at 1.805 GHz with a return loss of 13.708851 dB. The standard procedure is followed to obtain the impedance bandwidth (VSWR < 2) of 25.4%. Table 2.6 gives the performance parameters of the conventional PIFA systems.





**Fig. 2.25** 3-D polar plot ( $\phi = 90$ ) of the conventional PIFA structure

The design of PIFA with PBG structure is shown in Fig. 2.27. The PBG structure in this section is formed by some cylindrical air gaps, which are fixed on the Teflon substrate. The PBG structure has been designed using cylindrical air gaps over a dielectric substrate in a hexagonal pattern. Although the cylindrical air gaps has been placed periodically, the feed probe area has been kept blank i.e. without cylindrical air gaps to avoid the effect of feed probe. The dimension of the designed cylindrical air gap has diameter  $d = 3$  mm and periodicity i.e. the distance between cylindrical patch is  $a = 5$  mm. The finite element method (FEM)-based EM solver is used for simulation of PBG-based PIFA. The design and simulation results are shown in Figs. 2.28, 2.29, 2.30 and 2.31.

The PBG-based antenna's return loss characteristics are shown in Fig. 2.28, the antenna is resonating at 1.853 GHz. The standard procedure has been followed to obtain the impedance bandwidth ( $VSWR < 2$ ) of 39.9%. The obtained performance parameters for the PIFA system with PBG structure are given in Table 2.7. The simulated impedance bandwidth of the novel PBG-based PIFA is improved 14% than that of the conventional PIFA. The gain of the novel PBG PIFA is increased slightly.

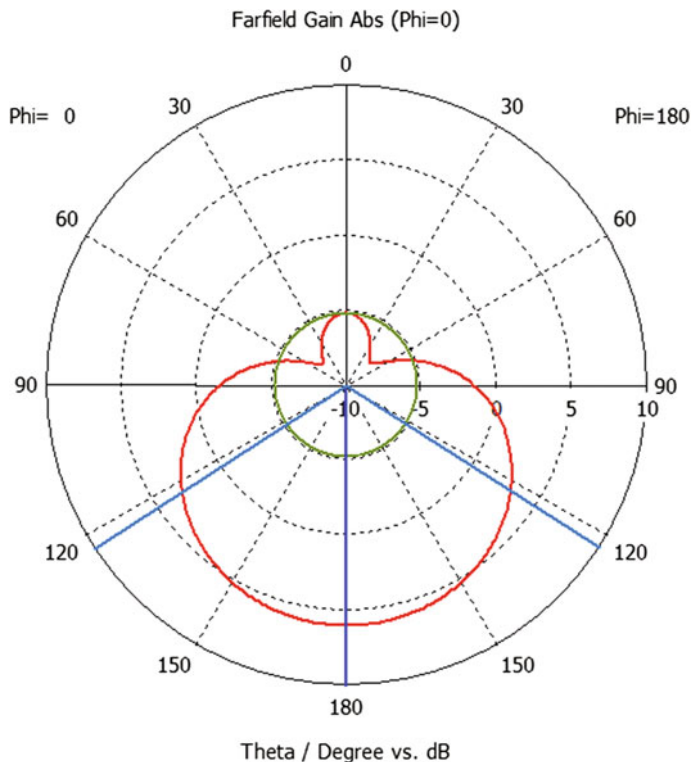
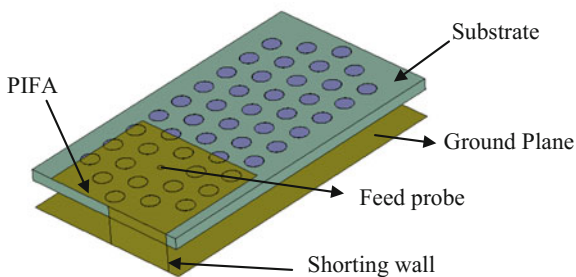


**Fig. 2.26** 3-D polar plot ( $\phi = 0$ ) of the conventional PIFA structure

**Fig. 2.27** Schematic of a PIFA system with PBG substrate



### 2.4.5 Procedure to Calculate Impedance Bandwidth

The performance of the antenna will be affected by high efficiency and large bandwidth parameters, which are interrelated to each other, and one does not have full freedom to separately set these parameters. The performance of an electrically small antenna can be examined in the same way as a simple resonator with the

**Table 2.5** Dimensions of PBG-based PIFA system

Parameter	Value (mm)
Width of the substrate	30
Length of the substrate, $L$	50
Width of the patch, $w$	24
Length of the patch, $l$	25
Distance of the feed in $x$ -axis, $f_x$	0
Distance of feed in $y$ -axis, $f_y$	15
Height of the substrate from ground, $h$	6
Thickness of the substrate, $T$	2

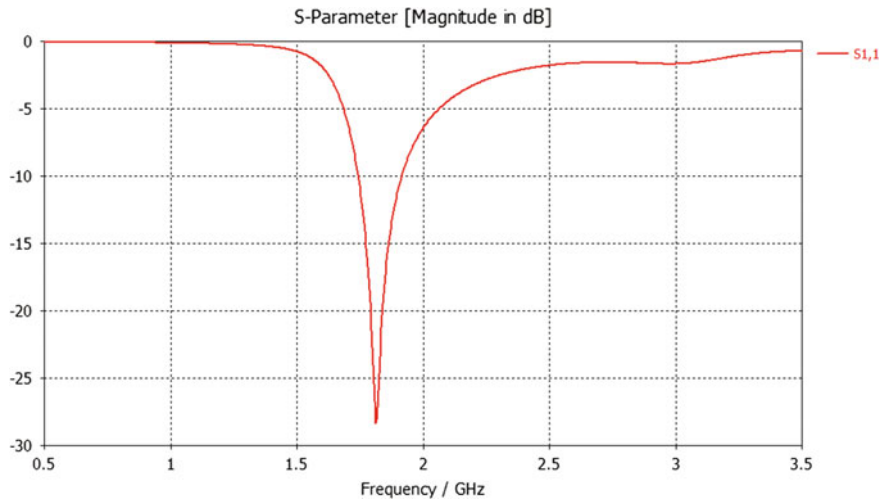


**Fig. 2.28** Return loss for the PIFA structure with PBG

**Table 2.6** Performance parameters of conventional PIFA system

Frequency	1.805 GHz
$S_{11}$	-13.70885 dB
Gain	5.871 dB
Directivity	5.851 dBi
Impedance bandwidth	25.4%

resonance frequency  $f_r$  and the quality factor  $Q$ . There are two losses in antenna, represented by external quality factor  $Q_e$  and unloaded quality factor  $Q_u$ . The total losses of antenna is represented by  $Q_l$  and is given by

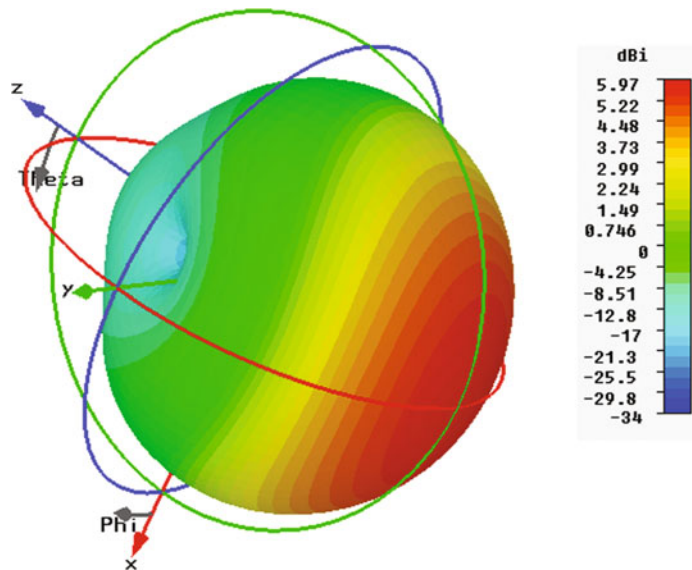
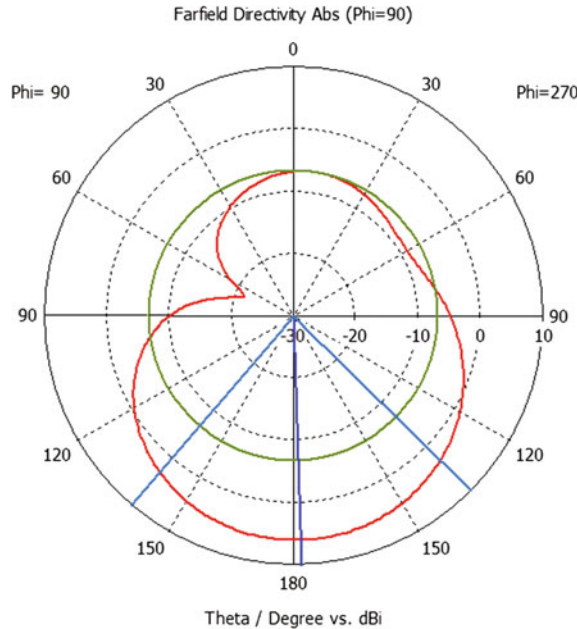
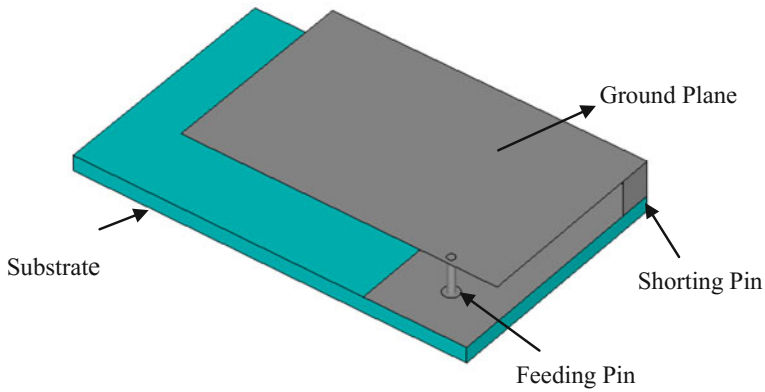
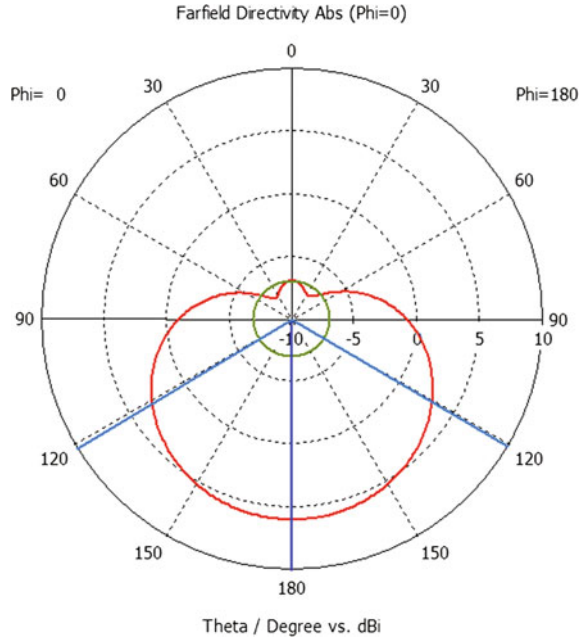


Fig. 2.29 Radiation pattern of PIFA structure with PBG

Fig. 2.30 Radiation pattern (in polar plot (phi = 90)) of the PIFA structure with PBG



**Fig. 2.31** Polar plot (phi = 0) of the PIFA structure with PBG



**Fig. 2.32** Schematic of conventional PIFA

$$Q_l = \frac{f_r}{B_{hp}} \quad (2.14)$$

where  $B_{hp}$  is the half-power bandwidth. The unloaded quality factor can be calculated by

**Table 2.7** Performance parameters of PBG-based PIFA system

Frequency	1.853 GHz
Return loss	−12.71 dB
Gain	5.990 dB
Directivity	5.971 dBi
Impedance bandwidth	39.9%

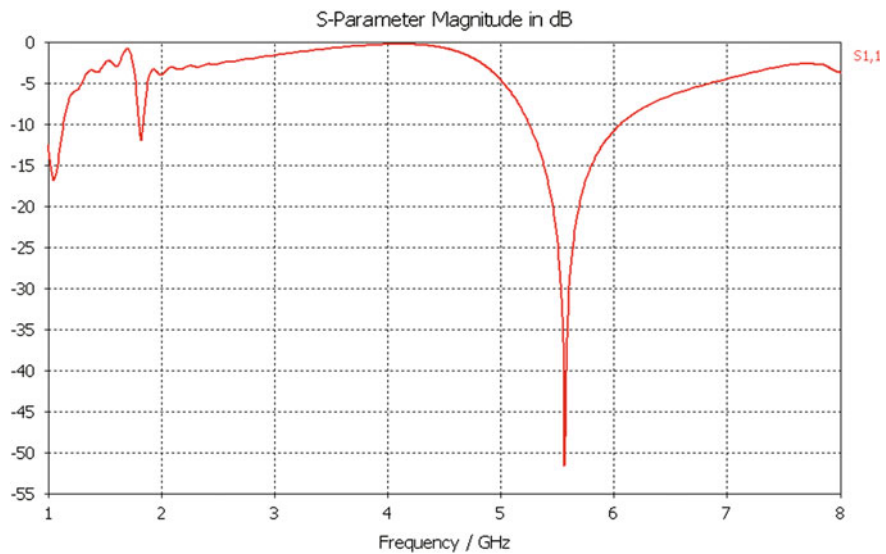


**Fig. 2.33** Return loss characteristics of a conventional PIFA

**Fig. 2.34** Radiation pattern of the conventional PIFA structure

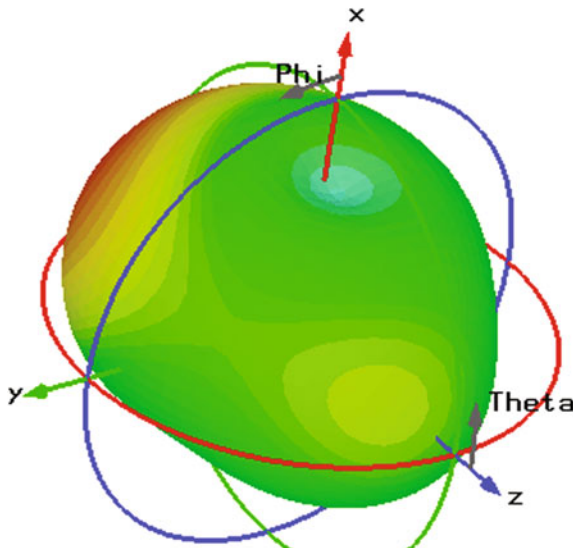


**Fig. 2.35** Radiation pattern (polar plot ( $\phi = 90^\circ$ )) of the conventional PIFA structure with metamaterials

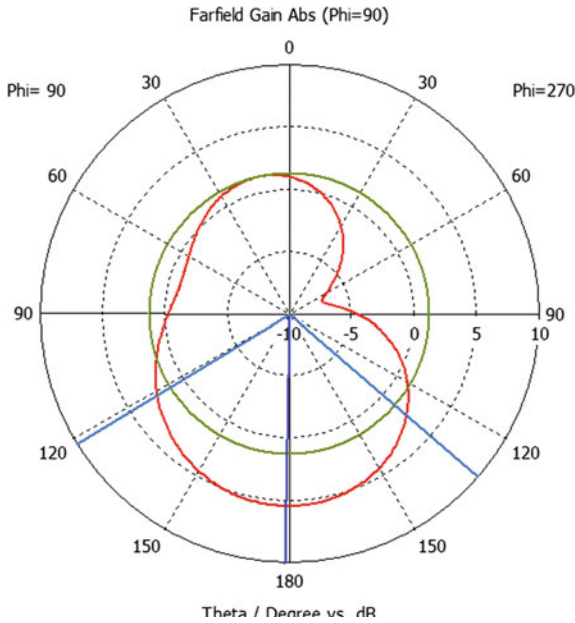


**Fig. 2.36** Radiation pattern (polar plot ( $\phi = 0^\circ$ )) of the conventional PIFA structure with metamaterials

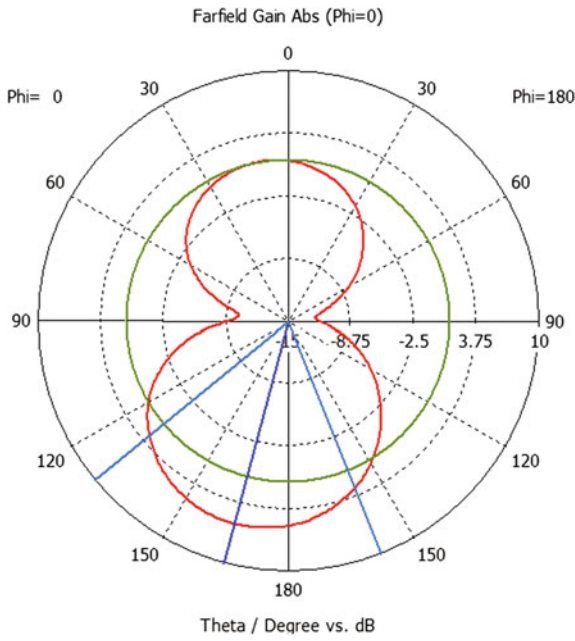


**Fig. 2.37** Design of metamaterial unit cell

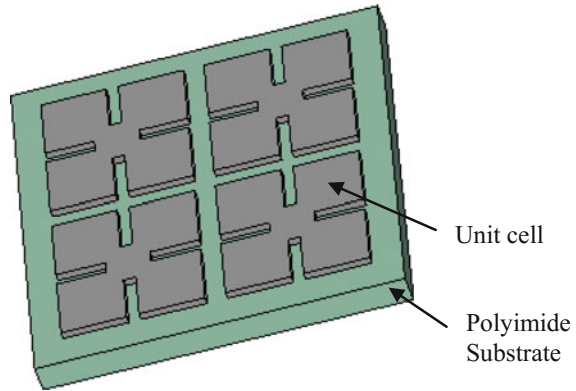


**Table 2.8** Dimensions of conventional PIFA system

Parameter	Value (mm)
Width of the substrate	30
Length of the substrate, $L$	50
Width of the patch, $w$	40
Length of the patch, $l$	25
Distance of the feed in $x$ -axis, $f_x$	6
Distance of feed in $y$ -axis, $f_y$	6.5
Height of the substrate from ground, $h$	4.5
Thickness of the substrate, $T$	2

$$Q_u = \frac{2 * Q_l}{1 \pm \rho(f_r)} \quad (2.15)$$

where the plus or minus sign refers to under- or over-coupled antenna, respectively, and  $\rho(f_r)$  is the reflection coefficient at resonance frequency. At critical coupling, Eq. (2.15) is reduced to

$$Q_u = 2 * Q_l \quad (2.16)$$

The unloaded quality factor is a physical constant and specific to each antenna structure. Thereby, it is not affected by coupling, and the impedance bandwidth for matching criterion  $VSWR \leq S$  can be given by

$$\text{Bandwidth(BW)} = \frac{S - 1}{Q_u * S} \quad (2.17)$$

This equation assumes critical coupling although the maximum bandwidth is obtained with a slight over-coupling. In Eq. (2.17),  $S$  is the standing wave ratio and assumed as 2. The measured voltage standing wave ratio should be less than  $S$ .



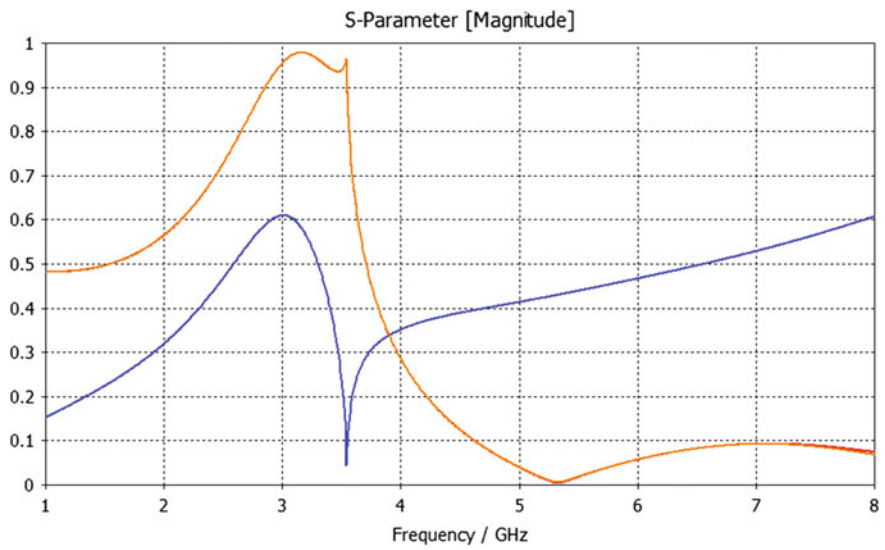


Fig. 2.38 Scattering parameters of SRR

**Table 2.9** Performance parameters of conventional PIFA system

Frequency	5.564 GHz
S <sub>11</sub>	−51.57 dB
Gain	3.252 dB
Directivity	4.670 dBi

The main intention behind the PIFA system with metamaterials is to downsize the antenna system. The FEM-based solver is used to design the antenna system and study the characteristics of a metamaterial-loaded antenna so as to compare its results with the conventional PIFA. The structure of the regular PIFA is shown in Fig. 2.32.

The planar inverted-F antenna (PIFA) consists of a substrate, radiating patch, ground plane shorting wall and feed. The dielectric constant of a substrate is 2.25. Copper material is used as the radiating patch, shorting wall, feed and ground plane. The dimensions of the substrate are 50 × 30 mm, respectively. The thickness of the polyimide substrate is 2 mm. The length and width of the ground plane are 13 and 30 mm, respectively. The height of the shorting wall is 4.5 mm and is placed in order to achieve impedance matching. The radiating patch is placed above the ground plane having dimensions of 40 and 25 mm, respectively. The FEM-based simulation software is used to simulate the PIFA. The feed has to be placed in a proper position in such a way that it obtains good results. The detailed dimensions of the conventional PIFA are given in Table 2.8, and the simulation results are shown in Figs. 2.33, 2.34, 2.35 and 2.36.

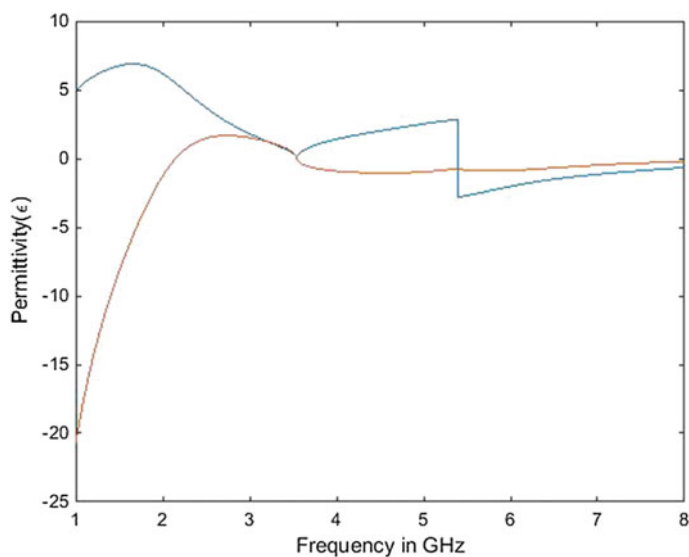


**Fig. 2.39** Permittivity characteristics of SRR

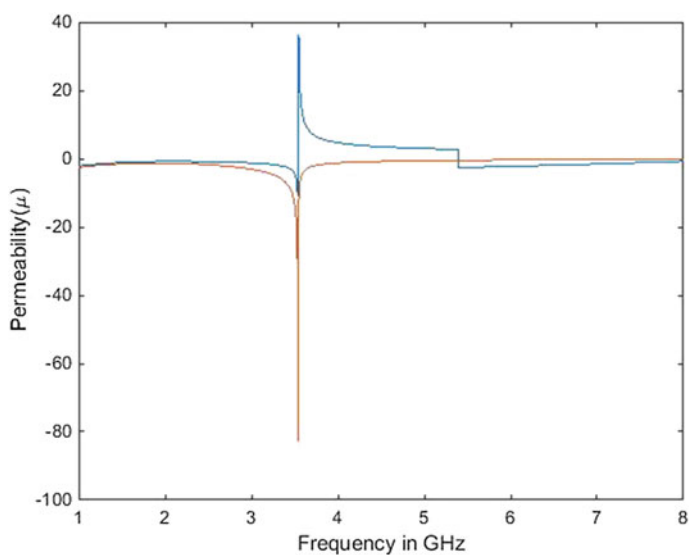


**Fig. 2.40** Permeability characteristics of SRR

The operating frequency range of PIFA system is 1–8 GHz. The center frequency is taken at minimum return loss, and the bandwidth can be calculated from return loss. The reflection coefficient of  $-51.57$  dB is obtained at a resonant

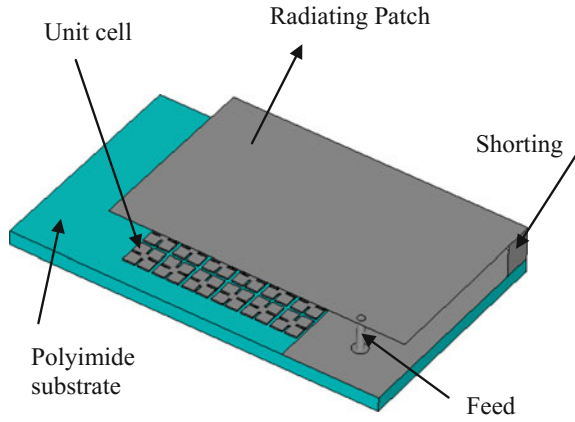


Fig. 2.41 Schematic of PIFA with metamaterial unit cell

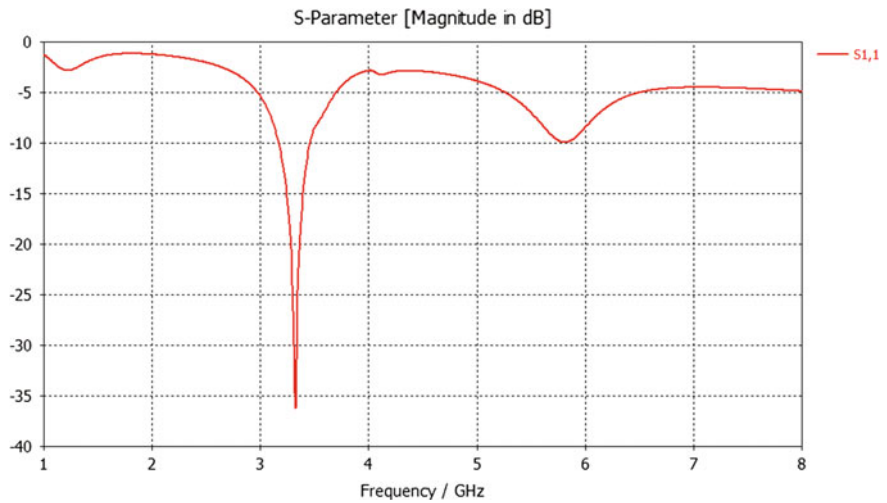


Fig. 2.42 Return loss characteristics of PIFA with metamaterial unit cell

frequency of 5.564 GHz for the designed dimensions of the antenna. The bandwidth of the antenna is found to be 23.28 MHz. The corresponding gain and directivity are 3.252 and 4.670 dBi. The obtained performance parameters for the conventional PIFA system are given in Table 2.9.

Numerical simulations are used to predict the transmission properties of SRRs. Here FEM-based solver is used to simulate the SRR structure. The simulations are done by propagating EM wave along  $z$ -direction. Vacuum was chosen as the background material. To validate the simulation, the SRR parameters were chosen

**Table 2.10** Dimensions of metamaterial unit cell

Parameter	Value (mm)
Height of the substrate, $h$	2
Metal thickness, $t$	0.2
Width of the unit cell	7.5
Length of unit cell	7.5
Gap in each part of unit cell, $g$	0.3
Gap between unit cell, $d$	0.5

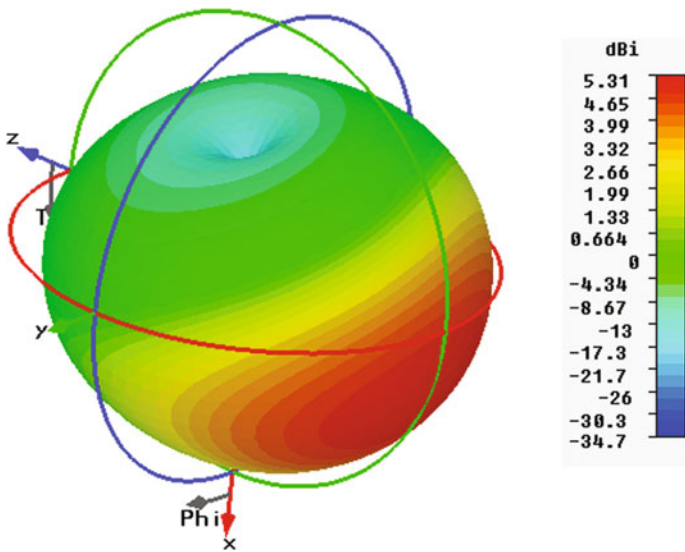


**Fig. 2.43** Radiation pattern of PIFA with metamaterial unit cell

to be  $d = 1.2$  mm,  $g = 0.3$  mm,  $w = 7.5$  mm and  $l = 7.5$  mm. The thickness and dielectric constant of the substrate were 0.75 and 2.23 mm, respectively. The thickness of unit cell is 0.2 mm. The unit cell is made up of copper material. The structure was then optimized for resonant frequency of 3 GHz, and the corresponding permittivity and permeability were extracted. Figure 2.37 shows the optimized structure of SRR, and the simulation results are shown in Figs. 2.38, 2.39 and 2.40. From the simulation results, it was seen that the designed square SRR metamaterial has negative parameters from 4 to 6 GHz. The dimensions of the designed metamaterial unit cell is given in Table 2.10.

The corresponding permittivity and permeability characteristics calculated using return loss are given below.

The design of PIFA with metamaterial unit cell is shown in Fig. 2.41. An array of SRRs is taken and placed on the substrate. The antenna is then scaled

**Fig. 2.44** Radiation pattern (polar plot ( $\phi = 90^\circ$ )) of PIFA structure with metamaterials

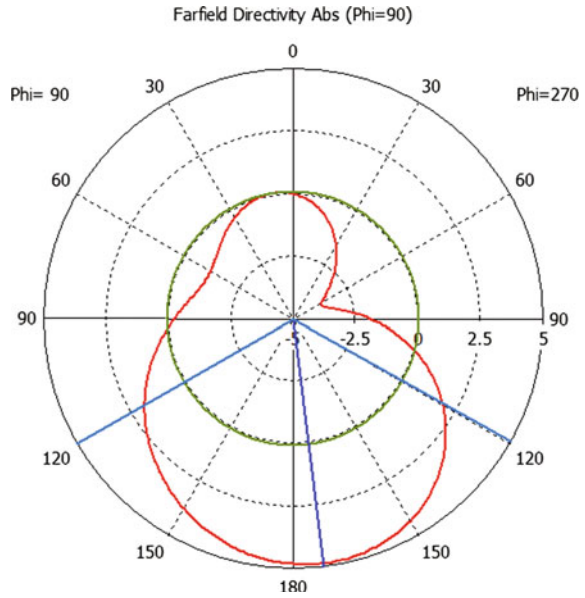
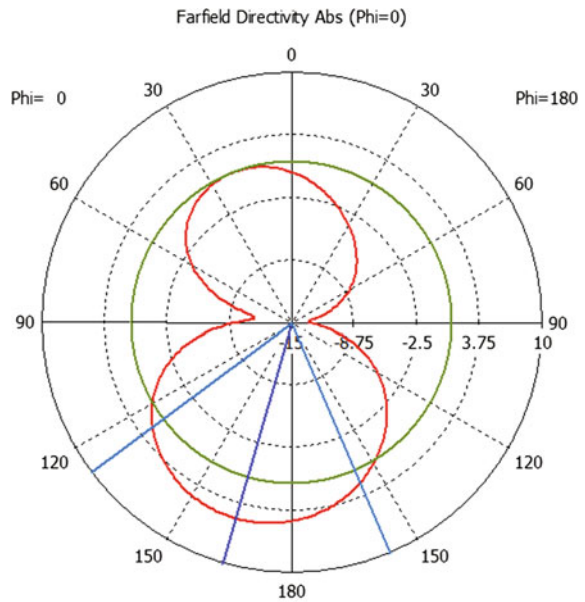


**Fig. 2.45** Radiation pattern (polar plot ( $\phi = 0^\circ$ )) of the PIFA structure with metamaterials



accordingly to resonate between 3 and 4 GHz frequencies. The design and simulations are done by FEM-based solver. The design and corresponding results are shown in Figs. 2.42, 2.43, 2.44 and 2.45.

**Table 2.11** Performance parameters of PIFA system with metamaterial unit cell

Frequency	3.324 GHz
$S_{11}$	-36.21248 dB
Gain	5.323 dB
Directivity	5.315 dBi

From simulation results, it can be shown that the PIFA system with metamaterials resonates at 3.324 GHz having reflection coefficient of -36.21 dB. The gain and directivity at 5.564 GHz are 5.323 dB and 5.315 dBi, respectively.

The deigned PIFA system without metamaterials resonates at a frequency of 5.564 GHz with return loss of 51.57 dB. The return loss, gain and directivity of PIFA with metamaterials are improved as compared to the conventional PIFA.

## 2.5 Conclusion

Planar inverted-F antennas are widely used in mobile systems because of its compact size and easy fabrication. These PIFA systems also find its application as wireless sensors that can be used in aircraft fuel tanks to check the fuel availability status. A technical review of advancements in design optimization of PIFA systems has been reported in this chapter. It has been observed that the antenna size can be further reduced by introducing metamaterial structures. In view of this, a metamaterial-loaded compact planar inverted-F antenna has been designed and simulated. The designed scattering parameter  $S_{11}$  of the metamaterial-based PIFA antenna is -51.57 dB, whereas that of the conventional PIFA is -12.893 dB only.

## References

1. Chi, P. L., R. Waterhouse, and T. Itoh, "Antenna miniaturization using slow wave enhancement factor from loaded transmission line models," *IEEE Transactions on Antennas and Propagation*, vol. 59, no. 1, pp. 48-59, Jan. 2011.
2. Kawano, Y., S. Hayashida, S. Bae, Y. Koyanagi and H. Morishita, "A study on miniaturization of 900 MHz and 2 GHz band antennas utilizing magnetic material," *2005 IEEE Antennas and Propagation Society International Symposium*, pp. 347-350 vol. 3B, 2005.
3. Karkkainen, M., S. Tretyakov, and P. Ikonen, "Numerical study of a PIFA with dispersive material fillings," *Microwave and Optical Technology Letters*, vol. 45, no. 1, pp. 5-8, Apr. 2005.
4. Xin-Yuan, L., F.J. Huil, Z. Kuang, H. Jun, and W. Qunl, "A compact wideband planar inverted-F antenna (PIFA) loaded with metamaterial," *Proceedings of IEEE Cross Strait Quad-Regional Radio Science and Wireless Technology Conference*, pp. 549-551, Jul. 2011.
5. Zuazola, I.J.G., J.C. Bachelor, and R.J. Langley, "Miniaturised multiband PIFA antenna using a frequency selective surface (FSS) ground plane," *Proceedings of IEEE Lough borough Antennas and Propagation Conference*, pp. 281-284, Apr. 2003.

6. Zhao, Y., Y. Hao, and C. G. Parini, "Radiation properties of PIFA on electromagnetic bandgap substrates," *Microwave and Optical Technology Letters*, vol. 44, no. 1, pp. 21–24, Jan. 2011.
7. Abidin Z. Z., Y. Ma, R. A. Abd-Alhameed, K. N. Ramli, D. Zhou, M. S. Bin-Melha, J. M. Noras, and R. Halliwell, "Design of 2 x 2 U-shape MIMO slot antennas with EBG material for mobile handset applications," *Progress in Electromagnetic Research, PIERS Online*, vol. 7, no. 1, pp. 81–84, 2011.
8. Attia, H., M. M. B. Suwailam, and O. M. Ramahi, "Enhanced gain planar inverted-F antenna with metamaterial superstrate for UMTS applications," *Proceedings of Progress in Electromagnetics Research Symposium*, pp. 494–497, Jul. 2010.
9. Pendry, J.B., A.J. Holden, W.J. Stewart, and I. Youngs, "Extreme Low Frequency Plasmons in Metallic Nano structures."
10. Lin, H. N., K. W. Lin, and S. C. Chen, "Use of frequency selective surface to prevent SAR and improve antenna performance of cellular phones," *Proceedings of Electromagnetics Research Symposium*, pp. 214–218, Sep. 2011.
11. Manapati, M. B. and R. S. Kshetrimayum, "SAR reduction in human head from mobile phone radiation using single negative metamaterials," *Journal of Electromagnetic Waves and Applications*, vol. 23, no. 10, pp. 1385–1395, 2009.
12. Faruque, M. R. I., M. T. Islam, and M. A. M. Ali, "A new design of metamaterials for SAR reduction," *Measurement Science Review*, vol. 13, no. 2, pp. 214–218, 2013.
13. Faruque, M. R. I., M. T. Islam, and N. Misran, "Analysis of electromagnetic absorption in mobile phones using metamaterials," *Electromagnetics*, vol. 31, no. 3, pp. 215–232, 2011.

## Suggested Bibliography

1. Baek S. and S. Lim, "Low-profile automotive antenna for omnidirectional vertical polarized signal reception," *Electromagnetics*, vol. 32, no. 8, pp. 481–494, 2012.
2. Chen, H. T., K. L. Wong, and T. W. Chiou, "PIFA with a meandered and folded patch for the dual-band mobile phone application," *IEEE Transactions on Antennas and Propagation*, vol. 51, no. 9, pp. 2468–2471, Sep. 2003.
3. Chen, J. H., Y. L. Ban, H. M. Yuan, and Y. J. Wu, "Printed coupled-fed PIFA for seven-band GSM/UMTS/LTE WWAN mobile phone," *Journal of Electromagnetic Waves and Applications*, vol. 26, pp. 390–401, 2012.
4. Dwivedi V., Y. P Kosta, R. Jyoti, and V. T. Patel, "An investigation on design and application issues of miniaturized compact microstrip patch antennas for RF wireless communication systems using metamaterials: A study," *Proceedings of IEEE International RF and Microwave Conference*, pp. 226–231, 2008.
5. Hao, Y., Y. Zhao, Y. J. Lee, and I. J Youngs, "Electrically small antennas with dielectric, magnetodielectric and metamaterial loading," *Proceedings of IEEE Loughborough Antennas and Propagation Conference*, pp. 57–62, Apr. 2007.
6. Ikonen, P. M. T., K. N. Rozanov, A. V. Osipov, P. Alitalo, and S. A. Tretyakov, "Magnetodielectric substrates in antenna miniaturization: Potential and limitations," *IEEE Transactions on Antennas and Propagation*, vol. 54, no. 11, pp. 3391–3399, Nov. 2006.
7. Jalal, A. S. A., A. Ismail, A. R. H. Alhawari, M. F. A. Rasid, N. K. Noordin, and M. A. Mahdi, "Miniaturized metal mount Minkowski fractal RFID TAG antenna with complementary split ring resonator," *Progress in Electromagnetics Research C*, vol. 39, pp. 25–36, 2013.
8. Jasik, H., (ed.), *Antenna Engineering Handbook*, New York, McGraw Hill, 1961.
9. Karkkainen, M., S. Tretyakov, and P. Ikonen, "Numerical study of a PIFA with dispersive material fillings," *Microwave and Optical Technology Letters*, vol. 45, no. 1, pp. 5–8, Apr. 2005.

10. Kulkarni, S. D. and S. N. Makarov, "A compact dual-band foam-based UHF PIFA," *Proceedings of IEEE Antennas and Propagation Symposium*, pp. 3609–3612, doi:[10.1109/APS.2006](https://doi.org/10.1109/APS.2006), Jul. 2006.
11. Lee, C. J., K. M. K. H. Leong, and T. Itoh, "Compact dual-band antenna using an anisotropic metamaterial," *Proceedings of The 36th European Microwave Conference*, pp. 1044–1047, 2006.
12. Lo, Y.T. and S.W. Lee, *Antenna Handbook* New York, Van Nostrand Reinhold, 1998.
13. Narayan S., Shamala J. B., R.U. Nair, and R.M. Jha, "Electromagnetic performance analysis of novel multi-band metamaterial FSS for millimeter wave applications," *TechScience Press Journal CMC: Computers, Materials & Continua*, vol. 729, p. 1–8, 2012. (Invited Paper).
14. Negative Refraction Metamaterials, *Fundamental Principles and Applications*. Wiley Interscience, A John Wiley and Sons, Inc., Publication.
15. Pintos, J. F., A. Louzir, P. Minard, J. Perraudeau, J. L. Mattei, D. Souriou, P. Queffelec, "Ultra-miniature UHF antenna using magneto-dielectric material," *IEEE International Symposium on Antenna Technology and Applied Electromagnetics and the American Electromagnetics Conference*, 4p., 2010.
16. Saraereh, O. A., M. Jayawardene, P. McEvoy, and J. C. Vardaxoglou, "Simulation and experimental SAR and efficiency study for a dual-band PIFA handset antenna (GSM 900/DCS 1800) at varied distances from a phantom head," *Technical Seminar on Antenna Measurements and SAR (AMS)*, pp. 5–8, doi:[10.1049/ic:20040066](https://doi.org/10.1049/ic:20040066), 2004.
17. Staub, O., J-F. Zurcher, A. Skrivervik, "Some considerations on the Correct Measurement of the Gain and Bandwidth of Electrically Small Antennas," *Microwave and Optical Technology Letter*, 17,3,February 201998,pp. 156–160.
18. Xiong, J., Y.F. Yu, Y.M. Liu, and X. Geng, "An electrically small planar loop antenna with high efficiency for mobile terminal applications," *Journal of Electromagnetic Waves and Applications*, vol. 26, pp. 744–756, 2012.



Metamaterial Inspired Electromagnetic Applications

Role of Intelligent Systems

Choudhury, B. (Ed.)

2017, XXVII, 173 p. 201 illus., Hardcover

ISBN: 978-981-10-3835-8